Bioscience, Biotechnology, and Biochemistry, 2021, Vol. 85, No. 5, 1077-1087

doi: 10.1093/bbb/zbab016
Advance access publication date: 1 February 2021
REGULAR PAPER

REGULAR PAPER

LncRNA small nucleolar RNA host gene 16 (SNHG16) silencing protects lipopolysaccharide (LPS)-induced cell injury in human lung fibroblasts WI-38 through acting as miR-141-3p sponge

Lei Xia,[1] Guoqing Zhu,[1] Haiyun Huang,[2] Yishui He,[3] and Xingguang Liu[2,*]

[1]Department of Pediatrics, Binzhou People's Hospital, Binzhou, Shandong, China; [2]Department of oral and maxillofacial surgery, School and Hospital of Stomatology, Cheeloo College of Medicine, Shandong University & Shandong Key Laboratory of Oral Tissue Regeneration & Shandong Engineering Laboratory for Dental Materials and Oral Tissue Regeneration, Jinan, Shandong, China; and [3]Department of Stomatology, Shenzhen Hospital of Southern Medical University, Shenzhen, China

*Correspondence: Xingguang Liu, qvnyls@163.com

ABSTRACT

Long noncoding RNA (LncRNA) small nucleolar RNA host gene 16 (SNHG16) is correlated with cell injuries, including pneumonia. However, its role and mechanism remain vague in pneumonia. The interplay among genes was confirmed by dual-luciferase reporter assay, RNA immunoprecipitation, and RNA pull-down assay. SNHG16 and sushi domain containing 2 (SUSD2) were upregulated, and miRNA (miR)-141-3p was downregulated in the serum of acute pneumonia patients and lipopolysaccharide (LPS)-challenged human lung fibroblasts WI-38. LPS induced apoptosis, autophagy, and inflammatory response in WI-38 cells, which was significantly attenuated by SNHG16 knockdown and/or miR-141-3p overexpression. Notably, both SNHG16 and SUSD2 were identified as target genes of miR-141-3p. Besides, the suppressive role of SNHG16 knockdown in LPS-induced in WI-38 cells was partially abolished by miR-141-3p silencing, and the similar inhibition of miR-141-3p overexpression was further blocked by SUSD2 restoration. In conclusion, knockdown of SNHG16 could alleviate LPS-induced apoptosis, autophagy, and inflammation in WI-38 cells partially though the SNHG16/miR-141-3p/SUSD2 pathway.

Graphical Abstract

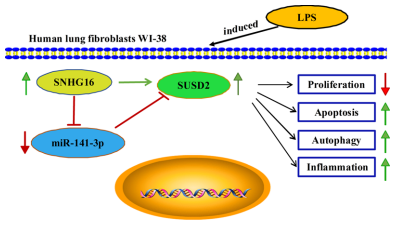

Received: 27 September 2020; **Accepted:** 21 January 2021

Blocking SNHG16 sponged miR-141-3p to modulate SUSD2 expression in the regulation of LPS-induced model of acute pneumonia in human lung fibroblasts WI-38.

Keywords: SNHG16, miR-141-3p, LPS, SUSD2, pneumonia

Infantile pneumonia is an inflammatory disease in lower respiratory tracts of infants infected with pathogens (Rudan *et al.* 2008). It is characterized by fever, cough, short breath and difficult breath. The occurrence of infantile pneumonia is commonly ascribed to bacteria, virus and mycoplasma infection (Dagan *et al.* 2011). Even though most cases have a good prognosis, pneumonia carries about 17% mortality rate in children in Mainland China (Guan *et al.* 2010). Thus, exploring new biomarker and therapeutic target of infantile pneumonia is urgently needed. Lipopolysaccharide (LPS) is a potent endotoxin from gram-negative bacteria, and can induce severe cell injury such as inflammatory response (Kagan 2017). Thereby, LPS-induced lung fibroblasts are a popular cell model of pneumonia to study the pathogenesis and pharmaceutical effect of drugs (Su *et al.* 2016).

Long noncoding RNAs (lncRNAs) are linear long transcripts more than 200 nucleotides, and participate in epigenetic regulation instead of protein coding (Lee 2012). Interaction with other noncoding RNA subtypes such as microRNAs (miRNAs) and small RNAs (siRNAs), lncRNAs are critical regulators in pathophysiologic processes and cellular functions, such as cell proliferation, metastasis, apoptosis, autophagy, and inflammatory response (Liu and Liu 2016). A pool of key lncRNAs have been identified in pneumonia using sequencing (Huang *et al.* 2016). This finding suggests that lncRNAs are also correlated with the progression of pneumonia through modulating functional genes. Small nucleolar RNA host gene 16 (SNHG16) is a recently identified member of SNHGs. However, SNHG16 has been gaining great attention in human diseases, including cancer and pneumonia (Zhang *et al.* 2019). For example, it has been well-documented about the association between SNHG16 and cell injuries in fibroblasts, myocardia and neurons (Liu, Chen and Zhu 2019; Xin *et al.* 2019; Zhou *et al.* 2019). However, the detail role of SNHG16 in human fibroblasts during pneumonia is largely undiscovered.

MiRNAs are short transcripts in length of approximate 22 nucleotides. It is well known that there was a lncRNA–miRNA–messenger RNA (mRNA) axis underlying the molecular mechanism of lncRNAs in regulating cell progression. Physically, miRNAs regulate functional genes expression via directly binding to 3′ untranslated region (3′UTR) of recipient mRNAs. Recently, miRNA expression files have been established in the serum of pneumonia patients (Owen *et al.* 2015; Lin *et al.* 2016; Huang *et al.* 2018; Wu *et al.* 2019), and abundant miRNAs are suggested to be biomarkers for the diagnosis and prognosis of pneumonia (Wu *et al.* 2019). MiRNA (miR)-141-3p has been implicated with LPS-induced cell injuries in rheumatoid arthritis, nonalcoholic steatohepatitis, neuropathic pain, as well as in pneumonia (Shen *et al.* 2017; Tran *et al.* 2017; Li *et al.* 2019; Quan, Zhang and Xue 2019). Nevertheless, the prominent role of miR-141-3p in pneumonia has not been revealed thoroughly.

In this study, we aimed to detect expression of SNHG16 in acute pneumonia patient and LPS-induced human fibroblasts WI-38. Furthermore, the role and molecular mechanism of SNHG16 in apoptosis, autophagy and inflammation was validated through serving as miR-141-3p sponge to regulate sushi domain containing 2 (SUSD2), which is a surface marker for mesenchymal stem cells and takes vital role in cancers (Sugahara *et al.* 2007; Cousins, Dorien and Gargett 2018).

Materials and methods

Serum sample collection

The peripheral venous blood (3 mL) samples were collected from Binzhou People's Hospital, and this study was approved by the ethics committee of this hospital. A total of 35 acute pneumonia patients (age: range 0.5-12 year; 20 males and 15 females) and 18 healthy volunteers (age: range 0.5-12 year; 10 males and 8 females) were recruited, and the written informed consent was obtained from all of them. The serum samples were captured after the centrifugation of the blood, and then stored at −80 °C.

Cell culture and LPS stimulation

Human lung fibroblasts WI-38 (CCL-75) was originally from American Type Culture Collection (Manassas, VA, USA). WI-38 cells were incubated in Dulbecco's modified Eagle's medium (Gibco, Grand Island, NY, USA) containing 10% fetal bovine serum (Gibco) and in a condition of 5% CO_2 at 37 °C. Different doses of LPS (0, 4, 8, 16, 32, and 64 mg/L) were added in medium for 8 h when WI-38 cells reached 80% confluence. And, 16 mg/L of LPS was selected for further functional analysis. These WI-38 cells were performed within 3-10 passages, and the Certificate of STR Analysis on this WI-38 cell line at 12th passage after the first acquisition was presented in Supplementary document-1.

Real-time reverse transcription-polymerase chain reaction (RT-qPCR)

Total RNA was isolated from serum and WI-38 cells using TRIzol® LS Reagent (Invitrogen, Waltham, MA, USA), and the quantity and quality of RNA sample were measured by Nanodrop 2000 (Thermo Fisher Scientific, San Jose, CA, USA) and RNA denatured agarose gel electrophoresis (Figure S1). The complementary DNA (cDNA) was synthesized using RNA (OD260/280 ratio: 1.8-2.1; 28S/18S ratio: 2.0-2.5), oligo(dT) and random primer (Thermo Fisher Scientific), and Omniscript RT kit (Qiagen, Hilden, Germany). The reverse transcription system was presented in Table S1, and the RNA samples were examined by RNA denatured agarose gel electrophoresis. A volume of 1/4 cDNA was used to analyze RNA expression with SYBR Premix Ex Taq TM II (Takara, Kusatsu, Japan). The PCR amplification system was presented in Table S2, and the melting curve and amplification curve were presented in Supplementary document-2. The special primers including SNHG16 (ENSG00000163597; forward 5′-TGGCTGTGGCCTTGAAAACA-3′ and reverse 5′-ACACCGTGGCTACTAGAGGA-3′; 144 nucleotides), miR-141-3p (forward 5′-GGTCCTAACACTGTCTGGTAAAGATGG-3′, and reverse 5′- TGGTGTCGTGGAGTCG-3′; 71 nucleotides), SUSD2 mRNA (forward 5′-CAGCTACCAGAGATGGCGAG-3′, and

reverse 5′-CCTCTCGGAAGTCATCGCTC-3′; 134 nucleotides), glyceraldehyde-phosphate dehydrogenase (GAPDH) mRNA (forward 5′-GACAGTCAGCCGCATCTTCT-3′, and reverse 5′-GCGCCCAATACGACCAAATC-3′; 104 nucleotides), and U6 mRNA (forward 5′-TGCGGGTGCTCGCTTCGGCAGC-3′, and reverse 5′-CCAGTGCAGGGTCCGAGGT-3′; 106 nucleotides). The GAPDH was used as internal control for SNHG16 and SUSD2, and U6 was for miR-141-3p. The standard curve of each primer pair has been drawn, and amplification efficiency (E) was calculated by $E = 10^{-1/\text{slope}}$ formula (Figure S2). Relative RNA expression was calculated by threshold cycle (Ct) values using $2^{-\Delta\Delta Ct}$ method.

Cell apoptosis analysis

Cell apoptosis was assessed by cell viability and apoptosis rate using methyl thiazolyl tetrazolium (MTT) assay and flow cytometry, respectively. For MTT assay, WI-38 cells (2×10^4) were transferred in 96-well plate, and then treated with LPS (0, 4, 8, 16, 32, and 64 mg/L) for 8 h. The cells were incubated with serum-free medium with MTT (5 mg/mL, Invitrogen) for 4 h in 5% CO_2 at 37 °C. After discarding the medium, 100 μL dimethyl sulfoxide was added with shaking for 10 min. The absorbance was quantified with a microplate reader at 490 nm. The cell viability was reflected by optimal density values from 3 independent MTT assays normalized to control group.

For flow cytometry, WI-38 cells (2×10^6) in 6-well plate were treated with 16 mg/L of LPS for 8 h, and then collected to measure apoptosis rate using fluorescein isothiocyanate (FITC) Annexin V (RUO) Kit (Becton-Dickinson, Franklin Lakes, NJ, USA). After labeled with Annexin V-FITC (5 μL) and propidium iodide (PI; 5 μL) for 15 min in the dark, the cells were resuspended in binding buffer (500 μL), followed with analysis on flow cytometry. Generally, cells can be tracked from Annexin V FITC−/PI− (viable or no measurable apoptosis), to Annexin V FITC+/PI− (early apoptosis, membrane integrity is present), and finally to Annexin V FITC+/PI+ (end stage apoptosis and death). The movement of cells through these 3 stages suggests apoptosis. Thus, apoptosis rate was assessed by the proportion of cells in Annexin V+/PI and Annexin V+/PI + quadrants.

Cell autophagy analysis

Autophagy was evaluated by the protein expression of LC3 and P62 using western blotting. First of all, total protein was isolated from the serum and WI-38 cells using Serum protein extraction kit (BestBio, Shanghai, China) and RIPA cell lysis buffer (Beyotime, Beijing, China), respectively. A total of 20 μg of protein samples were separated by sodium dodecyl sulfate-polyacrylamide gel electrophoresis, and transferred to polyvinylidene difluoride membranes (0.22 mm; Millipore, Bedford, MA, USA). After blocking, antibodies incubating and washing, the protein blots were visible with Pierce™ ECL Western blot substrate (Thermo Fisher Scientific). The primary antibodies including anti-LC3 (#2775, 1:1000), anti-P62 (#5114, 1:1000) and anti-GAPDH (#97 166, 1:1000) were purchased from Cell signaling technology (Danvers, Massachusetts, USA). GAPDH was the loading control of protein expression. The protein expression of LC3-II/LC3-I and P62 was calculated by gray density of protein bands compared to GAPDH according to Image J software (National Institutes of Health), and then normalized to control group. The data were the average of 3 independent western blotting analysis.

Inflammatory analysis

The inflammatory response was evaluated by the intracellular and extracellular expression of pro-inflammatory cytokines interleukin (IL)-6, IL-1β, and tumor necrosis factor (TNF)-α. In WI-38 cells and LPS-disposed WI-38 cells at 8 h, protein levels of IL-6, IL-1β, and TNF-α were measured by western blotting described above. The primary antibodies including anti-IL-6 (ab208113, 1:1000), anti-IL-1β (ab2105; 1:1000), and anti-TNF-α (ab6671, 1:2000) were purchased from Abcam (Cambridge, UK). The data was presented as fold change normalized to GAPDH. The protein expression of IL-6, IL-1β and TNF-α was calculated by gray density of protein bands compared to GAPDH according to Image J software (National Institutes of Health), and then normalized to control group. In the culture medium of WI-38 cells and LPS-disposed WI-38 cells at 8 h, productions of IL-6, IL-1β, and TNF-α were measured by special enzyme-linked immunosorbent assay (ELISA) using antibodies described as above. The procedures were carried out in according to the instruction. Cells of every group were treated with transfection or LPS in triplicate.

Cell transfection

For knockdown, siRNA against SNHG16 (si-SNHG16; sense 5′-UAUGAUAGCAGUAUGUUCCUU-3′ and antisense 5′-GGAACAUACUGCUAUCAUAGA-3′) and miR-141-3p inhibitor (anti-miR-141-3p; 5′-CCAUCUUUACCAGACAGUGUUA-3′) were provided by GenePharma (Shanghai, China), as well as their negative controls si-NC (sense 5′-CCTAACCACAAACTCTACGGC-3′ and antisense5′-CGUAGAGUUUGUGGUUAGGAC-3′) and anti-NC (5′-CAGUACUUUUGUGUAGUACAA-3′). For overexpression, miR-141-3p mimic (miR-141-3p; 5′-UAACACUGUCUGGUAAAGAUGG-3′) and its control miR-NC (5′-GUCCAGUGAAUUCCCAG-3′) were from GenePharma too. pcDNA3.1 vector was severally inserted with SNHG16 and the coding domain sequence of SUSD2 (NM_019601.4). The nucleotides were mixed with Lipofectamine 3000 (Invitrogen) at a final concentration of 2 μg (vectors) or 40 nM (oligonucleotides) for transfecting into WI-38 cells in 6-well plate. WI-38 cells reached 80% influence and in logarithmic phase prior to transfection. After transfection for 24 h, the cells were treated with LPS or collected for total RNA/protein analysis.

Identification of target binding

Dual-luciferase reporter assay and RNA immunoprecipitation (RIP) were performed to confirm the putative targeting binding between SNHG16 and miR-141-3p or between miR-141-3p and SUSD2 mRNA. Luciferase reporter vector pGL4 was selected to carry the wild type (WT) of the putative sequence on SNHG16 or SUSD2 3′UTR. Similarly, the mutant type (MUT) of them was constructed in pGL4 vector as well. The WI-38 cells in 24-well plate were cotransfected with 100 ng of SNHG16-WT/MUT and 30 nM of miR-141-3p/NC, or cotransfected with 100 ng of SUSD2 3′UTR-WT/MUT and 30 nM of miR-141-3p/NC. After transfection for 24 h, the double luciferase activities were detected using on Glo-Max LUMINOMETER (Promega, Madison, Wisconsin, USA). The data were presented as fold changes of the ratio of Firefly/Renilla luciferase activity with normalization to control group.

RIP assay was fulfilled using an EZ-Magna RIP kit (Millipore) in accordance to the manufacturer's direction. For RIP, WI-38 cells and 16 mg/L of LPS-treated WI-38 cells were lysed with RIP Lysis buffer, and the cell extracts were incubated with A/G

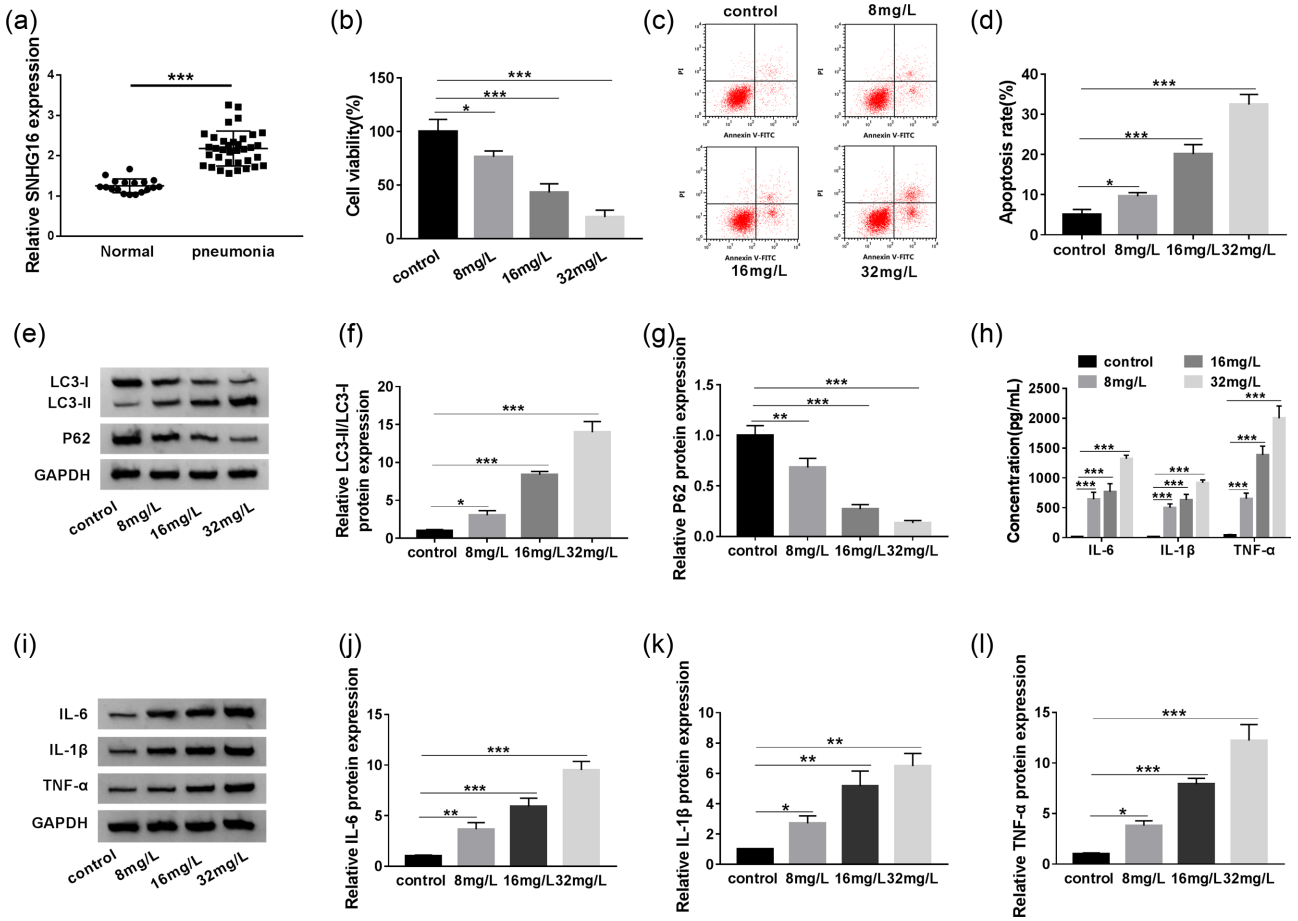

Figure 1. Small nucleolar RNA host gene 16 (SNHG16) was upregulated in acute pneumonia patients, and lipopolysaccharides (LPS)-induced cell injury in human lung fibroblast WI-38 cells. (a) Real-time reverse transcription-polymerase chain reaction (RT-qPCR) detected SNHG16 expression level in the serum of pneumonia patients (pneumonia; $n = 35$) and healthy individuals (normal; $n = 18$). (B-L) WI-38 cells were treated with 0, 8, 16 and 32 mg/L of LPS for 8 h. (b) methyl thiazolyl tetrazolium (MTT) assay tested cell viability. (c, d) Flow cytometry assessed apoptosis rate. (e-g) Western blotting evaluated autophagy-related proteins expression, and the protein bands of LC3-II/LC3-I and P62/glyceraldehyde-phosphate dehydrogenase (GAPDH) were quantified. (h) Enzyme-linked immunosorbent assay (ELISA) measured productions of interleukin (IL)-6, IL-1β, and tumor necrosis factor (TNF)-α in culture medium. (i-l) Western blotting evaluated expression of IL-6, IL-1β, and TNF-α in cells. * represents $P < .05$.

magnetic beads precovered with antibodies against Ago2 (ab32381, 1:50) or IgG (ab109761, 1:50). The precipitated RNA-protein complexes on the beads were treated with Proteinase K prior to RNAs isolation using TRIzol® LS (Invitrogen). For RNA pull-down assay, biotinylated SNHG16 and NC (Bio-SNHG16 and Bio-NC were established using T7 RNA polymerase (Promega) and biotinylated RNA-tagged mixtures (Roche, Basel, Switzerland), and WI-38 cells were transfected with Bio-SNHG16 or Bio-NC. The cell lysates were collected for incubation of Steptavidin MagnetSphere Paramagnetic beads (Promega) for 6 h at 4 °C. Then, the RNA samples from RIPs and pull-down products were isolated by TIRzol reagent, followed with RT-qPCR analysis.

Statistical analysis

The results were shown as the means ± SE from 3 independent data. SPSS 17.0 software (SPSS Inc., Chicago, IL, USA) was the platform to analyze the differences between 2 groups using two-tailed Student's *t*-test, or among groups using one-way analysis of variance. The *P* value less than 0.05 was considered as statistically significant.

Results

SNHG16 was upregulated in the serum of acute pneumonia patients

We collected the serum of pneumonia patients ($n = 35$) and healthy individuals ($n = 18$), and expression of SNHG16 was investigated. As shown in Figure S1, we obtained good quality of total RNA samples. And, the level of SNHG16 was significantly higher in pneumonia patients than normal controls (Figure 1a). This suggested a potential role of SNHG16 in pneumonia-mediated cell injury.

Silencing of SNHG16-alleviated LPS-induced WI-38 cell apoptosis, autophagy, and inflammation

To explore the role of SNHG16 in pneumonia, human lung fibroblasts WI-38 were exposed to LPS to mimic lung cell injury. After LPS treatment, cell viability of WI-38 cells was gradually suppressed at concentrations of 4, 8, 16, 32, and 64 mg/L, paralleled with control cells without LPS treatment (Figure S3 and Figure 1b). Flow cytometry showed that apoptosis rate was

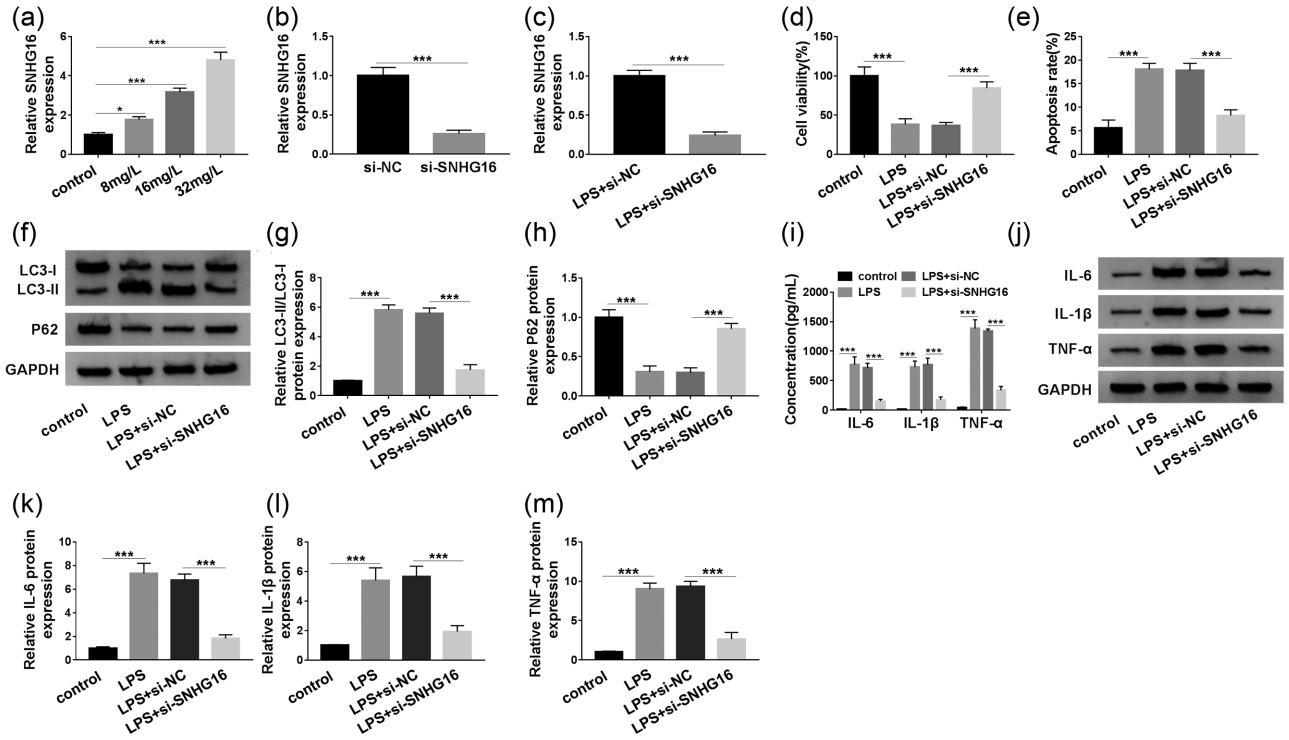

Figure 2. Expression and role of SNHG16 in LPS-induced WI-38 cells. (a, b) RT-qPCR-detected SNHG16 expression level in (a) WI-38 cells treated with 0, 8, 16, and 32 mg/L of LPS for 8 h, and (b) WI-38 cells transfected with siRNA against SNHG16 (si-SNHG16) or its negative control (si-NC) for 24 h. (c-m) WI-38 cells transfected with si-SNHG16 or si-NC were treated with 16 mg/L of LPS treatment for 8 h. (c) RT-qPCR detected SNHG16 level. (d, e) MTT assay and flow cytometry tested cell viability and apoptosis rate, respectively. (f-h) Western blotting evaluated LC3 and P62 expression levels. (i-m) IL-6, IL-1β, and TNF-α levels were measured by (i) ELISA in culture medium, and (j-m) Western blotting in cells. * represents $P < .05$.

increased with concentration of LPS in WI-38 cells (Figure 1c and d), suggesting cell apoptosis was stimulated. Western blotting data clarified that expression of LC3-II/LC-I was largely upregulated, and P62 was downregulated in WI-38 cells under treatment of 8-32 mg/L LPS (Figure 1e-g), indicating autophagy of WI-38 cells was induced. Secretions of pro-inflammatory cytokines IL-6, IL-1β and TNF-α were overall elevated in LPS-challenged WI-38 cells according to ELISA data (Figure 1h), accompanied with higher expression of IL-6, IL-1β and TNF-α (Figure 1i-l). These data collectively demonstrated that LPS could induce cell apoptosis, autophagy and inflammatory response in WI-38 cells, suggesting a lung cell injury elicited by LPS. Next, the expression of SNHG16 in LPS-challenged WI-38 cells was identified. Expectedly, the SNHG16 level was distinctively upregulated after 8-32 mg/L of LPS treatment for 8 h in a certain of dose-dependent manner (Figure 2a).

Thereby, role of SNHG16 was monitored in WI-38 cells under 16 mg/L of LPS treatment. First of all, we obtained a desired transfection efficiency of si-SNHG16 in WI-38 cells treated with LPS or not, as described by lower level of SNHG16 (Figure 2b and c). Then, LPS-induced cell viability inhibition and apoptosis rate promotion were attenuated when SNHG16 downregulation (Figure 2d and e). Highly promoted autophagy-related LC3-II/LC-I and inhibited P62 in LPS-challenged WI-38 cells were reversed due to silencing of SNHG16 (Figure 2f-h). The increase of extracellular concentration and intracellular expression of IL-6, IL-1β, and TNF-α in response to LPS was partially, but significantly inhibited by si-SNHG16 transfection (Figure 2i-m). These results showed that silencing of SNHG16 could alleviate LPS-induced cell apoptosis, autophagy and inflammation in WI-38 cells. Contrarily, overexpression of SNHG16 could induce WI-38 cell injury by promoting apoptosis rate and levels of LC3-II/LC3-I, IL-6, IL-1β, and TNF-α, as well as inhibiting P62 expression (Figure S4A-D).

SNHG16 functioned as a sponge for miR-141-3p

To identify molecular mechanism of SNHG16, target miRNAs were researched with bioinformatic software. As shown in Figure 3a, putative targeting sequence of miR-141-3p on SNHG16 was predicted on starbase (http://starbase.sysu.edu.cn/SNHG16-mir-141-3p), and luciferase reporter assay and RIP were utilized to confirm this potential complementary binding. Dual-luciferase reporter assay indicated that the luciferase activity of vectors containing SNHG16-WT was decreased in WI-38 cells transfected with miR-141-3p mimic (Figure 3b); whereas, SNHG16-MUT altered little difference on luciferase activity whenever ectopic expression of miR-141-3p or not. RIP assay revealed that SNHG16 and miR-141-3p were simultaneously enriched in Ago2-RIP of WI-38 cells and LPS-challenged WI-38 cells (Figure 3c and Figure S5A); besides, miR-141-3p was enriched in Bio-SNHG16-mediated pull-down product (Figure 3d). These findings suggested a direct binding relationship between SNHG16 and miR-141-3p. Expression of this miRNA was also detected in pneumonia samples using RT-qPCR. As a result, miR-141-3p level was downregulated in the serum of pneumonia patients ($n = 35$) and LPS-challenged WI-38 cells (Figure 3e and g). Moreover, Spearman's rank correlation analysis confirmed an inverse correlation between SNHG16 and

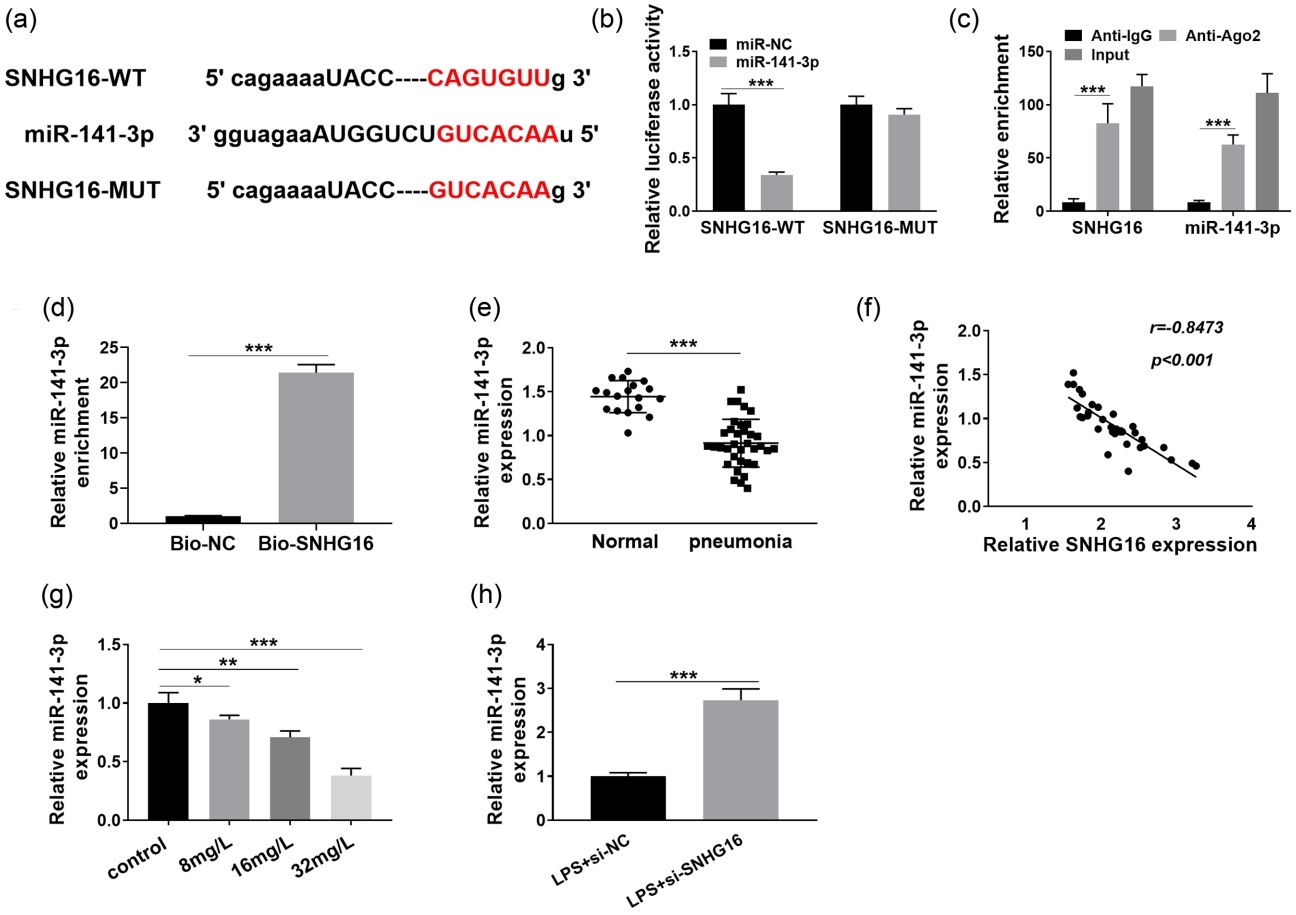

Figure 3. The interaction between SNHG16 and miRNA (miR)-141-3p, and the expression of miR-141-3p in acute pneumonia patients. (a) The putative binding sequence of miR-141-3p on SNHG16 and mutation sequence of SNHG16 were presented. (b) Dual-luciferase reporter assay examined the luciferase activity of vectors containing wild type or mutant type (WT or MUT) of SNHG16 (SNHG16-WT/MUT) in WI-38 cells transfected with miR-141-3p mimic (miR-141-3p) or its negative control (miR-NC). (c) SNHG16 and miR-141-3p levels were detected in RNA immunoprecipitation (RIP) with antibody against IgG or Ago2 (Anti-IgG/Ago2) from cell extract of WI-38 cells. (d) RNA pull-down assay detected miR-141-3p level in biotin-labeled SNHG16 (Bio-SNHG16) or Bio-NC mediated pull-down product. (e) RT-qPCR detected miR-141-3p expression level in the serum of pneumonia group ($n = 35$) and Normal group ($n = 18$). (f) Spearman's rank correlation analysis confirmed the correlation between SNHG16 and miR-141-3p expression. (g) RT-qPCR detected miR-141-3p level in WI-38 cells treated with 0, 8, 16, and 32 mg/L of LPS for 8 h. (h) RT-qPCR detected miR-141-3p level in WI-38 cells transfected with si-SNHG16 or si-NC for 24 h and then treated with 16 mg/L of LPS for 8 h. * represents $P < .05$.

miR-141-3p expression in this cohort of patients (Figure 3f). Meanwhile, silencing of SNHG16 led to miR-141-3p higher expression in LPS-treated WI-38 cells (Figure 3h). Collectively, we concluded that SNHG16 could function as miR-141-3p sponge in WI-38 cells.

Upregulation of miR-141-3p executed the inhibitory effect of SNHG16 knockdown on LPS-induced WI-38 cell injury

It was further analyzed about the effect of miR-141-3p on the role of SNHG16 knockdown in LPS-challenged WI-38 cells. WI-38 cells were transfected with si-SNHG16 alone or together with anti-miR-141-3p or anti-NC for 24 h prior to 16 mg/L of LPS treatment for 8 h. Transfection of anti-miR-141-3p caused great silence of miR-141-3p (Figure S6A), and this miR-141-3p downregulation could impair cell viability of WI-38 cells (Figure S6B). miR-141-3p was highly expressed in LPS-induced WI-38 cells with si-SNHG16 transfection, and this upregulation was cancelled with cointroduction with anti-miR-141-3p (Figure 4a). Rescue experiments indicated that the inhibitory effect of SNHG16 knockdown on cell apoptosis, autophagy and inflammation in WI-38 cells was partially counteracted when miR-141-3p was deleted, as evidenced by decreased cell viability (Figure 4b), and increased apoptosis rate (Figure 4c), higher LC3-II/LC-I level and lower P62 level (Figure 4d-f), improved expression and secretion of IL-6, IL-1β and TNF-α (Figure 4g-k). Therefore, miR-141-3p upregulation executed the inhibitory effect of SNHG16 knockdown on LPS-induced cell injury in WI-38 cells.

SUSD2 was a target gene of miR-141-3p

The downstream target gene of miR-141-3p was further predicted on starbase (http://starbase.sysu.edu.cn/miR-141-3p-susd2), and the putative binding site on SUSD2 3′UTR was presented in Figure 5a. Luciferase reporter assay and RIP analysis suggested a direct binding relationship between SUSD2 and miR-141-3p (Figure 5b and c and Figure S5B). Expression of this functional gene was also detected in pneumonia samples. RT-qPCR and western blotting data manifested that SUSD2 mRNA and protein levels were higher in the serum of pneumonia patients ($n = 35$) (Figure 5d and f). Moreover, there was an inverse

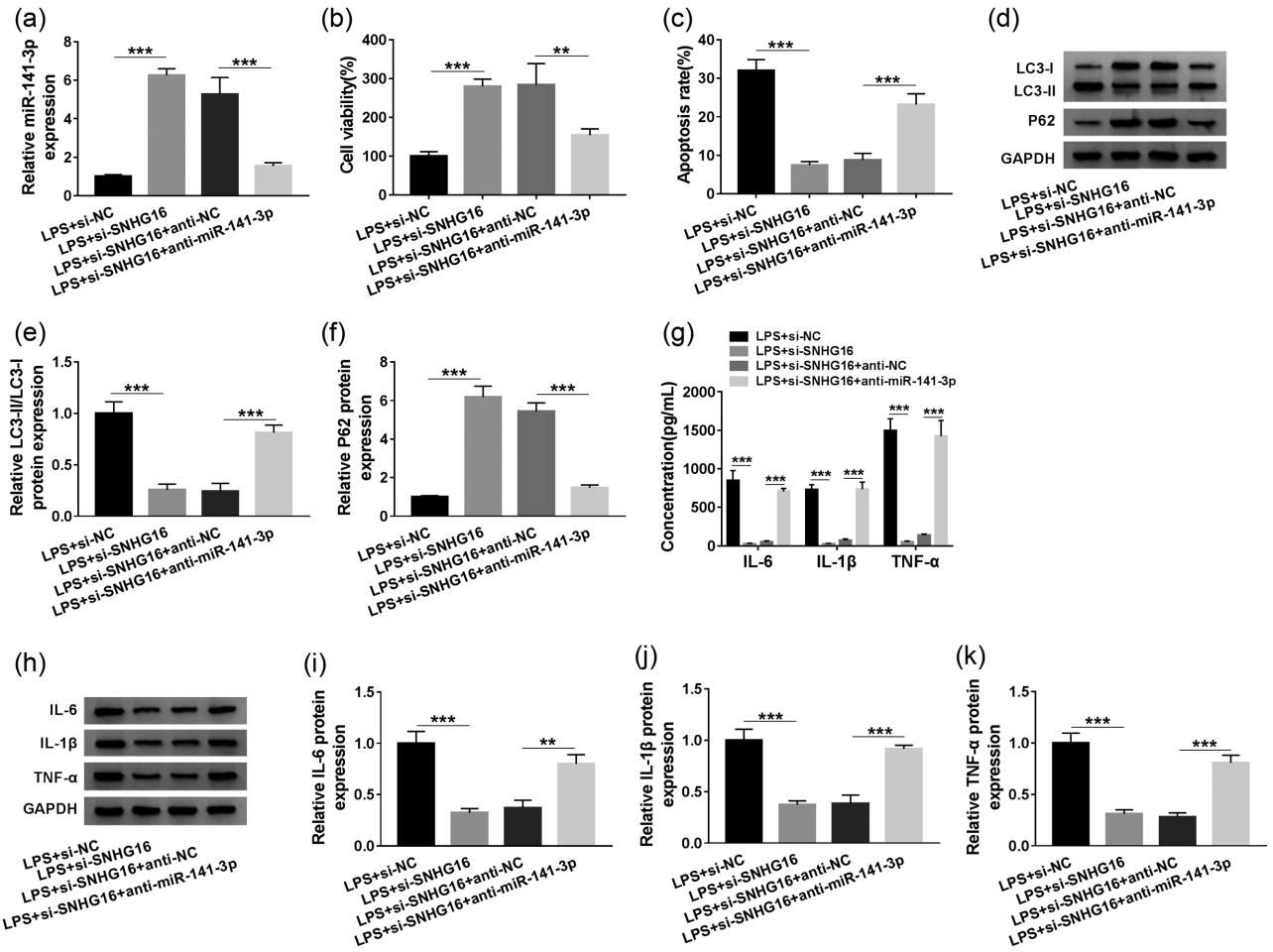

Figure 4. The effect of miR-141-3p expression on the inhibitory role of SNHG16 knockdown in LPS-challenged WI-38 cells. WI-38 cells were transfected with si-SNHG16 or si-NC, and cotransfected with si-SNHG16 and miR-141-3p inhibitor (anti-miR-141-3p) or its negative control (anti-NC) for 24 h prior to 16 mg/L of LPS treatment for 8 h. (a) RT-qPCR-detected miR-141-3p level. (b, c) MTT assay and flow cytometry tested cell viability and apoptosis rate, respectively. (d-f) Western blotting evaluated LC3 and P62 expression levels. IL-6, IL-1β, and TNF-α levels were measured by (g) ELISA in culture medium and (h-k) Western blotting in cells. * represents $P < .05$.

correlation between SUSD2 mRNA and miR-141-3p expression in this cohort of patients according to Spearman's rank correlation analysis (Figure 5e). Meanwhile, SUSD2 was highly induced by 8-32 mg/L of LPS treatment for 8 h in WI-38 cells as well (Figure 5g). These outcomes validated SUSD2 as a downstream target of miR-141-3p.

MiR-141-3p overexpression could protect WI-38 cells from LPS-induced cell apoptosis, autophagy, and inflammation through downregulating SUSD2

In addition, LPS-challenged WI-38 cells were pretransfected with miR-141-3p mimic alone or combined with pcDNA3.1-SUSD2 or pcDNA3.1 empty vectors for 24 h. The overexpression of miR-141-3p induced low expression of SUSD2 in LPS-treated WI-38 cells, and SUSD2 level was rescued in the presence of pcDNA3.1-SUSD2 vectors (Figure 6a). Similar to SNHG16 knockdown, miR-141-3p overexpression raised cell viability (Figure 6b), but depressed apoptosis rate (Figure 6c), reversed LC3-II/LC-I and P62 expression (Figure 6d-f), and inhibited IL-6, IL-1β and TNF-α expression and secretions in LPS-stimulated WI-38 cells (Figure 6g-k). These outcomes recommended a protective effect of miR-141-3p upregulation on LPS-induced cell apoptosis, autophagy and inflammatory response. Meanwhile, the ectopic expression of SUSD2 evidently rescued SUSD2 expression in miR-141-3p-overexpressed WI-38 cells under LPS stimulation, and further diminished the effects of miR-141-3p overexpression on the apoptosis, autophagy and inflammation in (Figure 6b-k). Therefore, miR-141-3p could protect WI-38 cells from LPS-induced cell injury through downregulating its target gene SUSD2. Additionally, it was also observed that si-SNHG16 transfection could downregulate SUSD2 expression via miR-141-3p (Figure 7a and b). Taken together, we proposed that SNHG16 knockdown functioned a protective role in LPS-induced WI-38 cell injury through miR-141-3p/SUSD2 axis.

Discussion

Pneumonia had been evidenced as an inflammation- and innate immune-correlated disease stimulated by microbial pathogens. During pneumonia, dysregulation of lncRNAs was a popular molecular pathology. For example, lncRNA NEAT1 was recognized to promote inflammasome activation in innate immune (Zhang *et al.* 2019), and NEAT1 inhibition could alleviate

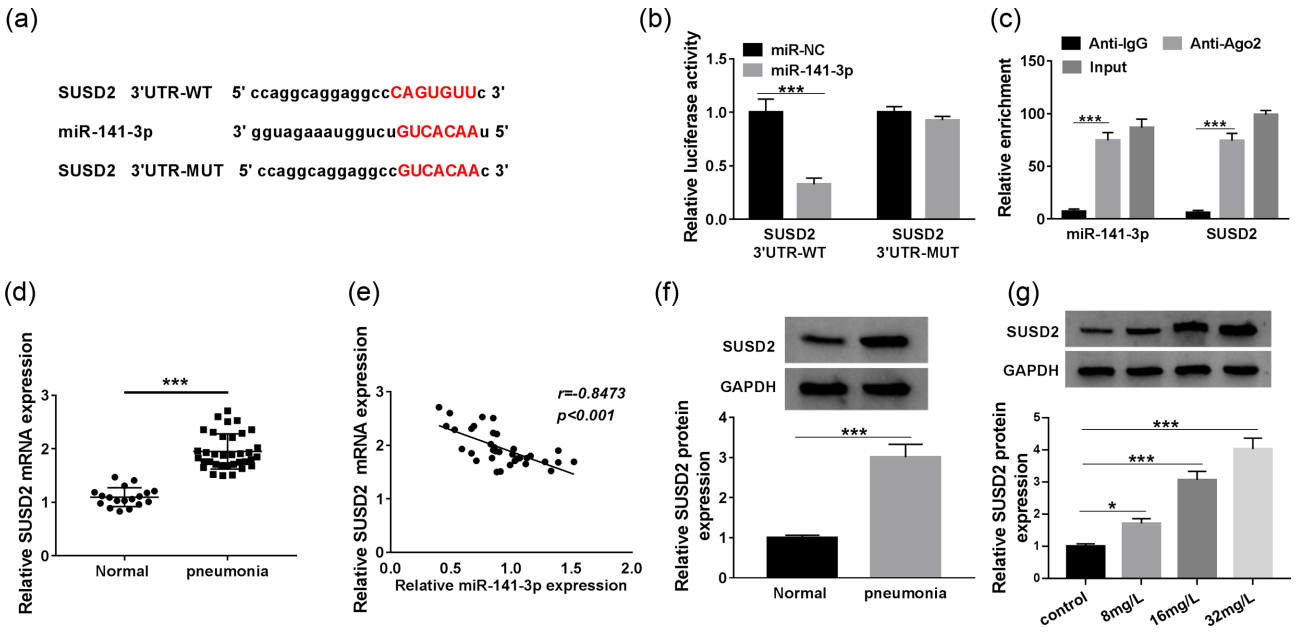

Figure 5. Sushi domain containing 2 (SUSD2) was a target gene of miR-141-3p. (a) The putative binding sequence of miR-141-3p on SUSD2 3′ untranslated region (3′UTR) and mutation sequence of SUSD2 3′UTR were presented. (b, c) Dual-luciferase reporter assay and RIP assays were used to determine the interplay between miR-141-3p and SUSD2 3′UTR in WI-38 cells. (d) RT-qPCR detected SUSD2 message RNA (mRNA) level in the serum of pneumonia patients ($n = 35$) and healthy individuals (Normal, $n = 18$). (e) Spearman's rank correlation analysis confirmed the correlation between SUSD2 mRNA and miR-141-3p expression. (f, g) Western blotting detected SUSD2 protein level in pneumonia patients' sera and WI-38 cells treated with 0, 8, 16, and 32 mg/L of LPS for 8 h. * represents $P < .05$.

inflammation and apoptosis of WI-38 cells induced by LPS through miR-193a-3p/Toll like receptor 4 (TLR4)/NF-κB pathway (Nong 2019). Moreover, multiple other lncRNAs including MALAT1, MIAT2, and CRNDE were implicated in LPS-evoked inflammatory injury in WI-38 cells (Zhu-Ge, Yang and Jiang 2018; Zhang, Zhao and Shao 2020; Zhu and Men 2020). Herewith, we investigated the expression and biological role of SNHG16 in cell viability, apoptosis rate, autophagy and inflammatory cytokines release in LPS-disposed WI-38 cells via competing endogenous RNAs (ceRNA) network.

In this study, we observed an upregulation of SNHG16 in the serum of pneumonia patients, which was also previously reported (Zhou *et al.* 2019). Furthermore, SNHG16 dysregulation had been earlier noticed in several inflammation-related diseases, such as atherosclerosis, sepsis, as well as pneumonia (Wang *et al.* 2018; An *et al.* 2019; Zhou *et al.* 2019). These findings together strongly recommend a potential role of SNHG16 in cell injuries. In pneumonia, Zhou *et al.* (2019) proposed that SNHG16 silencing suppressed LPS-evoked WI-38 cell apoptosis rate, release of IL-6, IL-1β and TNF-α, expression of Bax and cleaved caspase-3/9 via miR-146a-5p/CCL5 axis and JNK and NF-κB signaling pathways. Here, the similar outcomes were captured about the effect of SNHG16 on cell viability, apoptosis rate and inflammatory cytokines production; moreover, the autophagy was detected, as well. Knockdown of SNHG16 could increase P62 expression, but decrease LC3-II/LC-I expression in LPS-disposed WI-38 cells, suggesting a suppressive effect of SNHG16 silencing on autophagy. Besides, SNHG16 had been very recently disclosed to be associated with cell autophagy through serving as pro- or antiautophagy in different cells (Liu, Chen and Zhu 2019; Liu *et al.* 2019). Mechanically, we discovered a novel miRNA miR-141-3p was sponged by SNHG16, and then modulated SUSD2 expression. However, whether NF-κB or JNK signaling pathway could be abnormally activated in SNHG16/miR-141-3p axis had not been elaborated in this present study. By the way, the appreciated NF-κB signal was documented to be affected by SNHG16 at least partially via miR-15a/16, miR-17-5p and miR-146a-5p (Wang *et al.* 2018; An *et al.* 2019; Zhou *et al.* 2019), and might via miR-141-3p as well.

Additionally, SNHG16 was highly induced in response to LPS stimulation in WI-38 fibroblasts. Previous studies demonstrated that TLR4 was the receptor for LPS (Hu *et al.* 2013; Mazgaeen and Gurung 2020), and 2 signaling cascades were sequentially activated in the plasma membrane involving TIRAP and MyD88 adaptor proteins and in early endosomes engaging TRAM and TRIF adaptor proteins (Ciesielska, Matyjek and Kwiatkowska 2020). Thus, the upregulation of SNHG16 might be regulated by TLR4 pathways in some ways, and this hypothesis should be further deciphered.

In lung inflammation, Xiao *et al.* (2015) early pointed out that miR-141-3p and miR-200a could not regulate LPS-induced lung inflammation in macrophages, while other miR-200a family members including miR-429 and miR-200b/c could. However, miR-141-3p was later detected to be downregulated in LPS-induced human lung fibroblast WI-38 cells (Quan, Zhang and Xue 2019). Besides, we discovered downregulation of miR-141-3p in the serum of pneumonia patients in clinic comparing to that in healthy controls. Functionally, we and Quan, Zhang and Xue (2019) obtained a highly similar results of miR-141-3p overexpression in LPS-induced cell viability inhibition, apoptosis and inflammatory response in WI-38 cells. The difference between these 2 studies was the mechanism underlying miR-141-3p. They concluded that miR-141-3p mitigated LPS-evoked WI-38 inflammation injury by upregulating NOX2 and inhibiting p38/NF-κB signal, and we asserted that miR-141-3p protected WI-38 cells from LPS-induced inflammation injury via directly downregulating SUSD2. Meanwhile, it is a pity that the impact of miR-141-3p/SUSD2 axis on NF-κB signal was unclear in this study. By the way, miR-141-3p was also declared to be linked with acute lung cell injury induced by paraquat (Jin *et al.* 2018). In

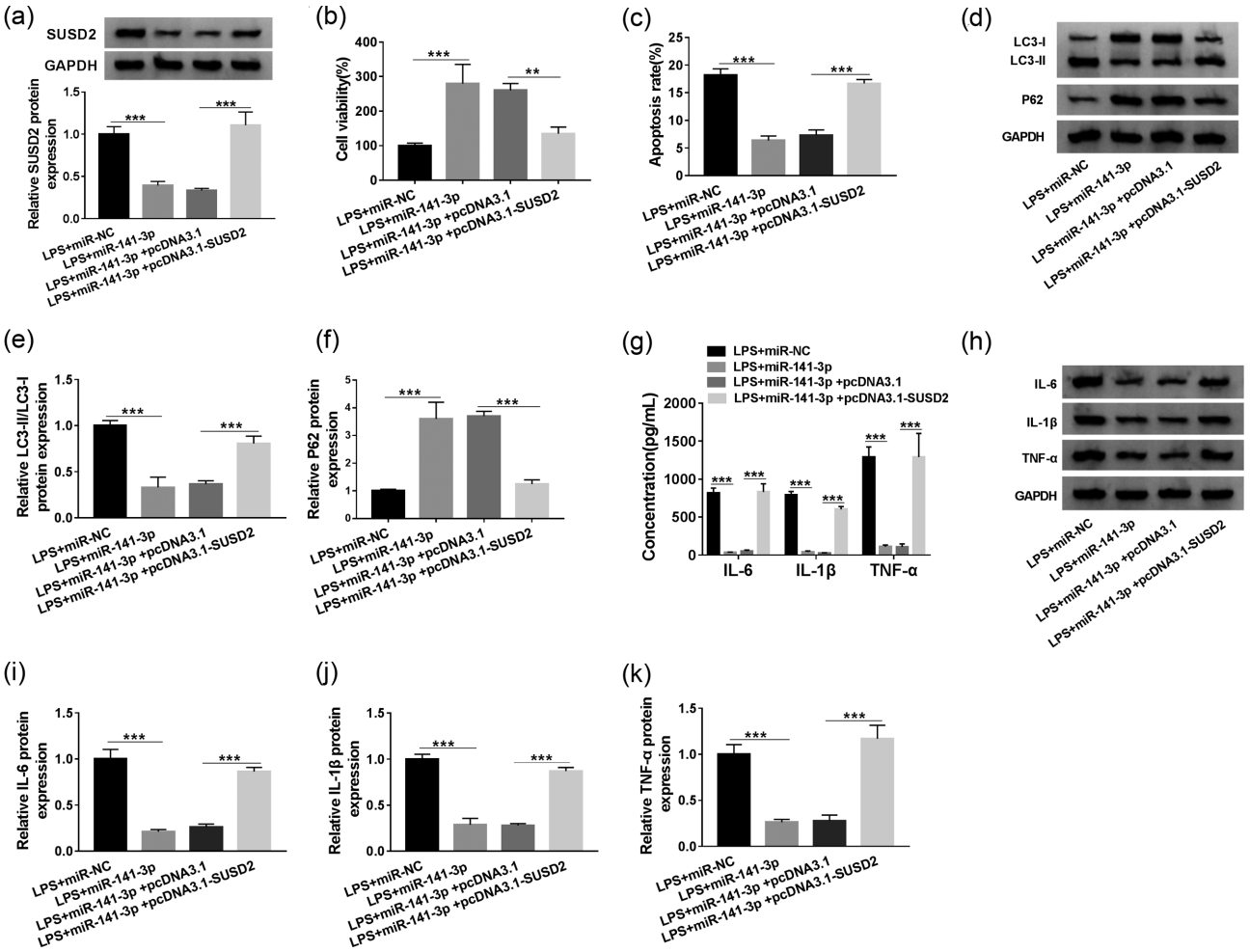

Figure 6. The effect of SUSD2 expression on miR-141-3p-mediated role in LPS-challenged WI-38 cells. WI-38 cells were transfected with miR-141-3p or miR-NC, and cotransfected with miR-141-3p and pcDNA3.1-SUSD2 or pcDNA3.1 empty vectors for 24 h prior to 16 mg/L of LPS treatment for 8 h. (a) Western blotting detected SUSD2 protein level. (b, c) MTT assay and flow cytometry tested cell viability and apoptosis rate, respectively. (d-f) Western blotting evaluated LC3 and P62 expression levels. IL-6, IL-1β and TNF-α levels were measured by (g) ELISA in culture medium, and (h-k) Western blotting in cells. * represents $P < .05$.

that research, downregulation of miR-141-3p underlay the protection of endothelial progenitor cells on paraquat-induced lung injury in mice. These outcomes together indicated a potent influence of miR-141-3p expression on lung injury, however, its role varied in different models of lung injury.

The role of SUSD2 in lung disorders including pneumonia remained vague, and field of miRNAs regulating SUSD2 was also considerably undeveloped. Here, we intended to uncover the contribution of SUSD2 to the role of SNHG16/miR-141-3p axis in pneumonia. The result was that SUSD2 expression was upregulated in the serum of pneumonia patients and LPS-induced WI-38 cells in a miR-141-3p-dependent manner. Upregulation of SUSD2 could facilitate LPS-induced cell injury, as evidenced by the promoted cell apoptosis, autophagy and inflammatory response in WI-38 cells with miR-141-3p-overexpression. Moreover, downregulation of SUSD2 was accompanied with the protective effect of SNHG16 knockdown and miR-141-3p overexpression in LPS-induced WI-38 cells. Therefore, we indicated a new role of SUSD2 in pneumonia via serving as a downstream target for miR-141-3p. By the way, SUSD2 was well-documented in different cancers, including breast cancer, colon cancer, cervical cancer, renal cell carcinoma, and lung cancer (Cheng *et al.* 2016), and SUSD2 could participate in cancer cell progression by miRNAs regulation (Umeh-Garcia *et al.* 2020), Galectin-1 interaction (Patrick and Egland 2019), Notch3 regulation (Xu *et al.* 2018), and Monocyte Chemoattractant Protein-1 upregulation (Hultgren *et al.* 2017).

Conclusion

Various ceRNA pathways and signaling pathways have been hidden in LPS-induced cell injury in fibroblasts in pneumonia, such as SNHG16/miR-146a-5p/CCL5 (Wang *et al.* 2018), XIST/miR-370-3p/TLR4 (Zhang *et al.* 2019), and HAGLROS/miR-100/NFKB3 axis (Liu *et al.* 2018). Here, we demonstrated SNHG16/miR-141-3p/SUSD2 as a novel ceRNA pathway in regulating fibroblast injury in pneumonia, and blocking SNHG16 or overexpressing miR-141-3p could suppress LPS-induced cell apoptosis, autophagy and inflammation in human fibroblasts WI-38.

Supplementary material

Supplementary material is available at *Bioscience, Biotechnology, and Biochemistry* online.

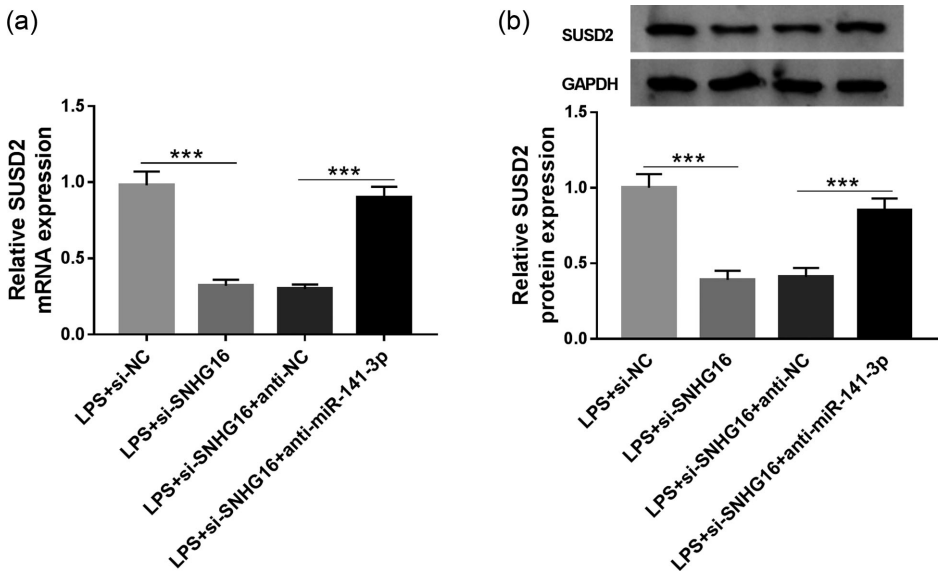

Figure 7. The role of SUSD2 in SNHG16/miR-141-3p axis in LPS-challenged WI-38 cells. (a, b) RT-qPCR and western blotting detected SUSD2 expression in WI-38 cells transfected with si-SNHG16 or si-NC, and cotransfected with si-SNHG16 and anti-miR-141-3p or anti-NC for 24 h prior to 16 mg/L of LPS treatment for 8 h. * represents $P < .05$.

Data availability statement

The original contributions presented in the study are included in the article/supplementary material, further inquiries can be directed to the corresponding author.

Author contribution

L.X. conceived the study. G.Z. and X.L. drafted the article. H.H. critically revised the article for important intellectual content. Y.H. and L.X. performed the statistical analysis. All authors have read and approved the article and agreed to be accountable for all aspects of the work in ensuring that questions related to the accuracy or integrity of any part of the work are appropriately investigated and resolved.

Funding

This work was supported by the Shandong Provincial Natural Science Foundation (Grant No. ZR2018PH027), Shandong Provincial Key Research and Development Plan (Grant No. 2019GSF108200), and Shandong Provincial Key Research and Development Plan (Grant No. 2018GSF118187).

Disclosure statement

No potential conflict of interest was reported by the authors.

References

An JH, Chen ZY, Ma QL *et al.* LncRNA SNHG16 promoted proliferation and inflammatory response of macrophages through miR-17-5p/NF-kappaB signaling pathway in patients with atherosclerosis. *Eur Rev Med Pharmacol Sci* 2019;**23**:8665-77.

Cheng Y, Wang X, Wang P *et al.* SUSD2 is frequently downregulated and functions as a tumor suppressor in RCC and lung cancer. *Tumour Biol* 2016;**37**:9919-30.

Ciesielska A, Matyjek M, Kwiatkowska K. TLR4 and CD14 trafficking and its influence on LPS-induced pro-inflammatory signaling. *Cell Mol Life Sci* 2020.

Cousins FL, Dorien FO, Gargett CE. Endometrial stem/progenitor cells and their role in the pathogenesis of endometriosis. *Best Pract Res Clin Obstet Gynaecol* 2018;**50**:27-38.

Dagan R, Bhutta ZA, de Quadros CA *et al.* The remaining challenge of pneumonia: the leading killer of children. *Pediatr Infect Dis J* 2011;**30**:1-2.

Guan X, Silk BJ, Li W *et al.* Pneumonia incidence and mortality in Mainland China: systematic review of Chinese and English literature, 1985-2008. *PLoS One* 2010;**5**:e11721.

Hu R, Xu H, Jiang H *et al.* The role of TLR4 in the pathogenesis of indirect acute lung injury. *Front Biosci* 2013;**18**:1244-55.

Huang F, Zhang J, Yang D *et al.* MicroRNA expression profile of whole blood is altered in adenovirus-infected pneumonia children. *Mediators Inflamm* 2018;**2018**:2320640.

Huang S, Feng C, Chen L *et al.* Identification of potential key long non-coding RNAs and target genes associated with pneumonia using long non-coding RNA sequencing (lncRNA-Seq): a preliminary study. *Med Sci Monit* 2016;**22**:3394-408.

Hultgren EM, Pa ME, Evans RL *et al.* SUSD2 promotes tumor-associated macrophage recruitment by increasing levels of MCP-1 in breast cancer. *PLoS One* 2017;**12**:e0177089.

Jin Y, Liu W, Liu X *et al.* Transplantation of endothelial progenitor cells attenuated paraquat-induced acute lung injury via miR-141-3p-Notch-Nrf2 axis. *Cell Biosci* 2018;**8**:21.

Kagan JC. Lipopolysaccharide detection across the kingdoms of life. *Trends Immunol* 2017;**38**:696-704.

Lee JT. Epigenetic regulation by long noncoding RNAs. *Science* 2012;**338**:1435-9.

Li G, Liu Y, Meng F *et al.* LncRNA MEG3 inhibits rheumatoid arthritis through miR-141 and inactivation of AKT/mTOR signalling pathway, *J Cell Mol Med* 2019;**23**:7116-20.

Lin J, Wang Y, Zou YQ *et al.* Differential miRNA expression in pleural effusions derived from extracellular vesicles of patients with lung cancer, pulmonary tuberculosis, or pneumonia. *Tumour Biol* 2016;**37**:15835-45.

Liu A, Liu S. Noncoding RNAs in growth and death of cancer cells. *Adv Exp Med Biol* 2016;**927**:137-72.

Liu H, Chen B, Zhu Q. Long non-coding RNA SNHG16 reduces hydrogen peroxide-induced cell injury in PC-12 cells by

up-regulating microRNA-423-5p. *Artif Cells Nanomed Biotechnol* 2019;**47**:1444-51.

Liu MH, Han T, Shi SM *et al*. Long noncoding RNA HAGLROS regulates cell apoptosis and autophagy in lipopolysaccharides-induced WI-38 cells via modulating miR-100/NF-κB axis. *Biochem Biophys Res Commun* 2018;**500**:589-96.

Liu Y, Gu S, Li H *et al*. SNHG16 promotes osteosarcoma progression and enhances cisplatin resistance by sponging miR-16 to upregulate ATG4B expression. *Biochem Biophys Res Commun* 2019;**518**:127-33.

Mazgaeen L, Gurung P. Recent advances in lipopolysaccharide recognition systems. *Int J Mol Sci* 2020;**21**:379.

Nong W. Long non-coding RNA NEAT1/miR-193a-3p regulates LPS-induced apoptosis and inflammatory injury in WI-38 cells through TLR4/NF-kappaB signaling. *Am J Transl Res* 2019;**11**:5944-55.

Owen HC, Torrance HD, Jones TF *et al*. Epigenetic regulatory pathways involving microRNAs may modulate the host immune response following major trauma. *J Trauma Acute Care Surg* 2015;**79**:766-72.

Patrick ME, Egland KA. SUSD2 proteolytic cleavage requires the GDPH sequence and inter-fragment disulfide bonds for surface presentation of Galectin-1 on breast cancer cells. *Int J Mol Sci* 2019;**20**:3814.

Quan B, Zhang H, Xue R. miR-141 alleviates LPS-induced inflammation injury in WI-38 fibroblasts by up-regulation of NOX2. *Life Sci* 2019;**216**:271-8.

Rudan I, Boschi-Pinto C, Biloglav Z *et al*. Epidemiology and etiology of childhood pneumonia, *Bull World Health Organ* 2008;**86**:408-16.

Shen WS, Xu XQ, Zhai NN *et al*. Potential mechanisms of microRNA-141-3p to alleviate chronic inflammatory pain by downregulation of downstream target gene HMGB1: in vitro and in vivo studies. *Gene Ther* 2017;**24**:353-60.

Su Y, Yao H, Wang H *et al*. IL-27 enhances innate immunity of human pulmonary fibroblasts and epithelial cells through up-regulation of TLR4 expression. *Am J Physiol Lung Cell Mol Physiol* 2016;**310**:L133-141.

Sugahara T, Yamashita Y, Shinomi M *et al*. Isolation of a novel mouse gene, mSVS-1/SUSD2, reversing tumorigenic phenotypes of cancer cells in vitro. *Cancer Sci* 2007;**98**:900-8.

Tran M, Lee SM, Shin DJ *et al*. Loss of miR-141/200c ameliorates hepatic steatosis and inflammation by reprogramming multiple signaling pathways in NASH. *JCI Insight* 2017;**2**:e96094.

Umeh-Garcia M, Simion C, Ho PY *et al*. A novel bioengineered miR-127 prodrug suppresses the growth and metastatic potential of triple-negative breast cancer cells. *Cancer Res* 2020;**80**:418-29.

Wang W, Lou C, Gao J *et al*. LncRNA SNHG16 reverses the effects of miR-15a/16 on LPS-induced inflammatory pathway, *Biomed Pharmacother* 2018;**106**:1661-7.

Wu X, Wu C, Gu W *et al*. Serum exosomal MicroRNAs predict acute respiratory distress syndrome events in patients with severe community-acquired pneumonia. *Biomed Res Int* 2019;**2019**:3612020.

Xiao J, Tang J, Chen Q *et al*. miR-429 regulates alveolar macrophage inflammatory cytokine production and is involved in LPS-induced acute lung injury. *Biochem J* 2015;**471**:281-91.

Xin B, Liu Y, Li G *et al*. The role of lncRNA SNHG16 in myocardial cell injury induced by acute myocardial infarction and the underlying functional regulation mechanism. *Panminerva Med* 2019. Online ahead of print.

Xu Y, Miao CY, Jin CJ *et al*. SUSD2 promotes cancer metastasis and confers cisplatin resistance in high grade serous ovarian cancer. *Exp Cell Res* 2018;**363**:160-70.

Zhang C, Ren X, He J *et al*. The prognostic value of long noncoding RNA SNHG16 on clinical outcomes in human cancers: a systematic review and meta-analysis. *Cancer Cell Int* 2019;**19**:261.

Zhang H, Zhao J, Shao P. Long noncoding RNA MIAT2 alleviates lipopolysaccharide-induced inflammatory damage in WI-38 cells by sponging microRNA-15. *J Cell Physiol* 2020;**235**:3690-7.

Zhang P, Cao L, Zhou R *et al*. The lncRNA Neat1 promotes activation of inflammasomes in macrophages. *Nat Commun* 2019;**10**:1495.

Zhang Y, Zhu YY, Gao GS *et al*. Knockdown XIST alleviates LPS-induced WI-38 cell apoptosis and inflammation injury via targeting miR-370-3p/TLR4 in acute pneumonia. *Cell Biochem Funct* 2019;**37**:348-58.

Zhou Z, Zhu Y, Gao G *et al*. Long noncoding RNA SNHG16 targets miR-146a-5p/CCL5 to regulate LPS-induced WI-38 cell apoptosis and inflammation in acute pneumonia. *Life Sci* 2019;**228**:189-97.

Zhu W, Men X. Negative feedback of NF-kappaB signaling by long noncoding RNA MALAT1 controls lipopolysaccharide-induced inflammation injury in human lung fibroblasts WI-38, *J Cell Biochem* 2020;**121**:1945-52.

Zhu-Ge D, Yang YP, Jiang ZJ. Knockdown CRNDE alleviates LPS-induced inflammation injury via FOXM1 in WI-38 cells. *Biomed Pharmacother* 2018;**103**:1678-87.